

# Optical frequency comb generation from a monolithic microresonator

P. Del'Haye,<sup>1</sup> A. Schliesser,<sup>1</sup> O. Arcizet,<sup>1</sup> T. Wilken,<sup>1</sup> R. Holzwarth,<sup>1</sup> and T.J. Kippenberg<sup>1,\*</sup>

<sup>1</sup>*Max Planck Institut für Quantenoptik, 85748 Garching, Germany*

Optical frequency combs[1, 2, 3] provide equidistant frequency markers in the infrared, visible and ultra-violet[4, 5] and can link an unknown optical frequency to a radio or microwave frequency reference[6, 7]. Since their inception frequency combs have triggered major advances in optical frequency metrology and precision measurements[6, 7] and in applications such as broadband laser-based gas sensing[8] and molecular fingerprinting[9]. Early work generated frequency combs by intra-cavity phase modulation[10, 11], while to date frequency combs are generated utilizing the comb-like mode structure of mode-locked lasers, whose repetition rate and carrier envelope phase can be stabilized[12]. Here, we report an entirely novel approach in which equally spaced frequency markers are generated from a continuous wave (CW) pump laser of a known frequency interacting with the modes of a monolithic high-Q microresonator[13] via the Kerr nonlinearity[14, 15]. The intrinsically broadband nature of parametric gain enables the generation of discrete comb modes over a 500 nm wide span ( $\approx 70$  THz) around 1550 nm without relying on any external spectral broadening. Optical-heterodyne-based measurements reveal that cascaded parametric interactions give rise to an optical frequency comb, overcoming passive cavity dispersion. The uniformity of the mode spacing has been verified to within a relative experimental precision of  $7.3 \times 10^{-18}$ . In contrast to femtosecond mode-locked lasers[16] the present work represents an enabling step towards a monolithic optical frequency comb generator allowing significant reduction in size, cost and power consumption. Moreover, the present approach can operate at previously unattainable repetition rates[17] exceeding 100 GHz which are useful in applications where the access to individual comb modes is required, such as optical waveform synthesis[18], high capacity telecommunications or astrophysical spectrometer calibration[19].

Optical microcavities[20] are owing to their long temporal and small spatial light confinement ideally suited for nonlinear frequency conversion, which has led to a dramatic improvement in the threshold of nonlinear optical light conversion[21]. In contrast to stimulated gain, parametric frequency conversion[22] does not involve coupling to a dissipative reservoir, is broadband as it does not rely on atomic or molecular resonances and constitutes a phase sensitive amplification process, making it uniquely suited for tunable frequency conversion. In the case of a material with inversion symmetry - such as silica - the non linear optical effects are dominated by the third order non linearity. The process is based on four-wave mixing among two pump photons (frequency  $\nu_P$ ) with a signal ( $\nu_S$ ) and idler photon ( $\nu_I$ ) and results in the emergence of (phase coherent) signal and idler sidebands from the vacuum fluctuations at the expense of the pump field (cf. Fig.1). The observation of parametric interactions requires two conditions to be satisfied. First momentum conservation has to be obeyed. This is intrinsically the case in a whispering gallery type microcavity[20] since the optical modes are angular momentum eigenstates and have (discrete) propagation constants  $\beta_m = \frac{m}{R}$  resulting from the periodic boundary condition, where the integer  $m$  designates the mode number and  $R$  denotes the cavity radius. Hence the conversion of two pump photons (propagation constant  $\beta_N$ ) into adjacent signal and idler modes ( $\beta_{N-\Delta N}$ ,  $\beta_{N+\Delta N}$ ,  $\Delta N = 1, 2, 3 \dots$ ) conserves mo-

mentum intrinsically[14] (analogous reasoning applies in the case where the two annihilated photons are in different modes, i.e. for four-wave mixing, cf. Fig. 1b). The second condition that has to be met is energy conservation. As the parametric process creates symmetrical sidebands with respect to the pump frequency (obeying  $h\nu_I + h\nu_S = 2h\nu_P$ , where  $h$  is the Planck constant) it places stringent conditions on the cavity dispersion that can be tolerated since it requires a triply resonant cavity. This is a priori not expected to be satisfied, since the distance between adjacent modes  $\nu_{\text{FSR}} = |\nu_m - \nu_{m+1}|$  (the free spectral range, FSR) can vary due to both material and intrinsic cavity dispersion which impact  $n_{\text{eff}}$  and thereby render optical modes (having frequencies  $\nu_m = m \cdot \frac{c}{2\pi R n_{\text{eff}}}$ , where  $c$  is the speed of light in vacuo) non-equidistant. Indeed, it has only recently been possible to observe these processes in microcavities (made of crystalline[15]  $\text{CaF}_2$  and silica[14, 23]).

Importantly, this mechanism could also be employed to generate optical frequency combs: the initially generated signal and idler sidebands can interact among each other and produce higher order sidebands (cf. Fig. 1) by non-degenerate four-wave mixing (FWM)[24] which ensures that the frequency difference of pump and first order sidebands  $\Delta\nu \equiv |\nu_P - \nu_S| = |\nu_P - \nu_I|$  is *exactly* transferred to all higher order sidebands. This leads to an equidistant spectrum throughout the *entire* comb. This can be readily seen by noting that e.g. the 2<sup>nd</sup> order sidebands are generated by mixing among the pump and first order signal/idler sidebands (e.g.  $\nu_{S2} = \nu_P + \nu_S - \nu_I = \nu_P - 2\Delta\nu$ ), which rigidly determines the spacing of any successively higher sidebands. Thus, provided the cavity exhibits low

\*Electronic address: tj.k@mpq.mpg.de

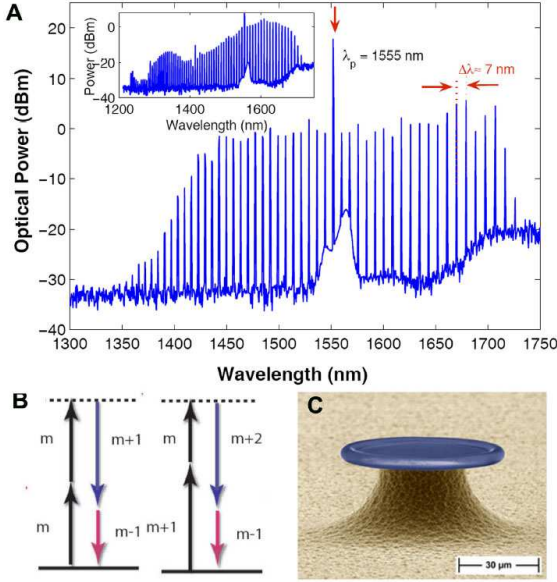


FIG. 1: Broadband parametric frequency conversion from a 75- $\mu\text{m}$ -diameter monolithic microresonator. Panel A: Spectrum of the parametric frequency conversion observed in an 75- $\mu\text{m}$ -diameter monolithic toroid microcavity when pumped with 60 mW continuous wave (CW) laser power at 1555 nm. The combination of parametric interactions and four-wave-mixing (FWM) gives rise to a broadband emission, spaced by the cavity free spectral range. Inset: Broadband parametric conversion of a different sample generating more than 70 parametric modes extending over a wavelength span of nearly 500 nm (launched power 130 mW). The asymmetry in the spectrum (with higher power in the higher wavelength sidebands) and the amplitude modulation of the emission is attributed to Raman amplification and variation of the taper fiber output coupling, respectively. Panel (B): Schematic of the processes that contribute to the parametric conversion: degenerate (left) and non-degenerate (right) four-wave-mixing among cavity eigenmodes. Momentum conservation is intrinsically satisfied for the designated angular mode number ( $m$ ) combinations. Panel (C): Scanning electron microscope image of a toroid microcavity on a silicon chip.

dispersion, the successive four-wave mixing to higher orders would intrinsically lead to the generation of phase coherent sidebands with equal spacing, *i.e.* an *optical frequency comb*. Here, we report that microresonators allow realization of this process and generation of optical frequency combs.

We employ ultra-high- $Q$  monolithic microresonators in the form of silica toroidal microcavities[13] on a silicon chip, which possess giant photon storage times ( $\tau$ ) *i.e.* ultra-high quality factors ( $Q = 2\pi\nu\tau > 10^8$ ) and small mode volumes. Highly efficient coupling is achieved using tapered optical fibers[25]. Owing to the high circulating power, parametric interactions are readily observed at a threshold of approx. 50  $\mu\text{W}$ . When pumping with a continuous wave (CW) 1550-nm laser source,

we observe a massive cascade and multiplication of the parametric sidebands extending to both higher and lower frequencies. Fig. 1a shows a spectrum in which a 75- $\mu\text{m}$ -diameter microcavity was pumped with 60 mW power, giving rise to an intra-cavity intensity exceeding 1  $\text{GW}/\text{cm}^2$ . The parametric frequency conversion could extend over more than 490 nm (cf. Fig 1a inset), with the total conversion efficiency being 21.2 % (The highest observed conversion efficiency was 83 % by working in the over-coupled regime[13]). These bright sidebands (termed Kerr combs in the remaining discussions) could be observed in many different samples. Also, in the largest fabricated samples (190  $\mu\text{m}$  diameter) 380-nm broad Kerr combs comprising 134 modes spaced by 375 GHz could be generated at the expense of slightly higher pump power (cf. Supplementary Information).

To verify that the Kerr comb indeed contains equidistant frequencies, we employed a fiber-laser based optical frequency comb[26] from Menlo Systems (termed “reference comb” in the remaining discussion) as a reference grid whose repetition rate is  $f_{\text{rep}} = 100$  MHz. The principle underlying our measurement is that the beating generated on a photodiode by superimposing the reference comb with the Kerr comb will produce beat notes which constitute a unique replica of the optical spectrum in the radio frequency domain, provided that the highest produced beat note in the detection process is  $< f_{\text{rep}}/2$  (cf. Fig. 2b), similar to multi-heterodyne frequency comb spectroscopy[27]. Specifically, if the Kerr comb is equidistant, the beat notes with the reference comb will constitute an equidistant comb in the RF domain (with frequency spacing  $\Delta f$ , where  $\Delta f = (\Delta\nu \bmod f_{\text{rep}})$ ). Fig. 2a shows the experimental setup for the optical beat measurement. In brief, an external cavity laser at 1550 nm was used as pump laser (cf. Fig 2 main panel). The Kerr lines of the microcavity were superimposed with the reference comb in a beat note detection unit (BDU), consisting of polarizing optics to combine the reference and Kerr combs and a grating to select the desired region of spectral overlap. In this manner, the beating of 9 simultaneously oscillating parametric modes (covering  $> 50$  nm of wavelength span) were recorded, as shown in Fig. 2c. Remarkably, from the equidistant spacing of the radio-frequencies, it is found that the generated sidebands are *equidistant* to within less than 5 kHz (as determined by the measurement time of 200  $\mu\text{s}$ ).

To improve the accuracy, we developed an additional experiment where we measured the beat-notes of three Kerr modes with the fiber-reference comb using three separate BDUs (cf. Fig. 3a) each counting a single beat of radio frequency ( $f_0, f_1, f_2$ ). A signal-to-noise ratio exceeding 30 dB in 500 kHz bandwidth was achieved, sufficient to use radio-frequency counters, which were all referenced to a 10 MHz reference signal provided by the MPQ hydrogen Maser. The beat-note measured on BDU1 was used to implement an offset lock between a

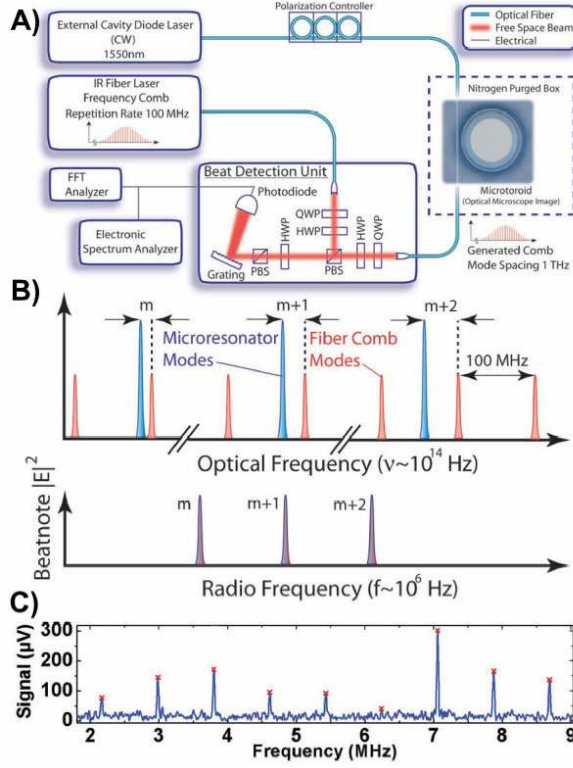


FIG. 2: Parametric beat note setup. Panel (A) shows the experimental setup consisting of an external cavity laser (ECL) coupled to an ultra-high-Q monolithic microresonator in a nitrogen environment via a tapered fiber. The parametric output is coupled into one port of a beat note detection unit (BDU). The second port of the BDU is coupled to a mode-locked femtosecond erbium doped fiber laser that serves as a reference comb. A grating is used to select a spectral region of the Kerr modes and a PIN Si photodiode records their beatings with the reference comb (See supplementary information for details). Panel (B) shows the measurement principle. The beating of the reference comb with the parametric lines yields beat frequencies in the radio-frequency domain. Panel (C): RF Spectrum of 9-simultaneously oscillating Kerr modes, exhibiting a uniform spacing.

single reference comb line and the pumping laser by a known offset frequency ( $f_0$ ). The second (third) counter measured the  $N^{\text{th}}$  ( $M^{\text{th}}$ ) mode of the Kerr comb as shown in Fig. 3. For equidistant mode spacing, the second (third) BDU gives rise to the beat frequency  $f_1 = f_0 + \Delta f \times N$  ( $f_2 = f_0 + \Delta f \times M$ ). The uniformity of the Kerr comb was then checked by comparing the variation in the mode spacing, i.e.  $\epsilon \equiv \frac{f_2 - f_1}{M - N} - \frac{f_1 - f_0}{N}$ . Alternatively, direct counting of the ratio  $(f_1 - f_0) / (f_2 - f_0) = \frac{N}{M}$  was implemented (using frequency mixing and ratio counting, cf. SI). Fig. 4b shows the result of this measurement (for  $N = 5$ ,  $M = 7$ ) and a counter gate time ( $\tau$ ) of 1 second and more than 3000 records. The scatter in the data follows a Gaussian distribution (and follows a  $\frac{1}{\sqrt{\tau}}$  dependence of the Allan deviation, cf. Fig. 4b). The

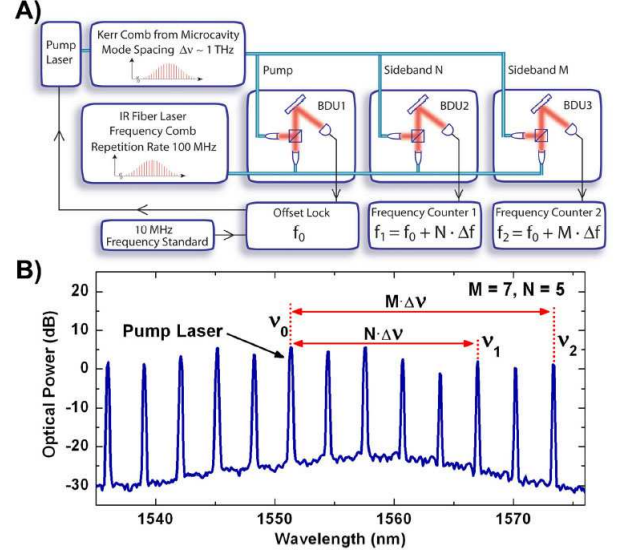


FIG. 3: Probing the equidistance of the comb structure. Panel (A): Simplified schematic of the setup which consists of three beat note detection units (BDUs) to measure the beating of three Kerr modes with the fiber based reference comb. All BDUs are referenced to the MPQ hydrogen Maser as frequency standard. The first BDU is used to implement a phase lock between one comb line of the reference comb and the pump laser (which constitutes one mode of the Kerr comb). Panel (B): The parametric spectrum under consideration for validating the equidistance of the comb modes.

cavity modes of this measurement span over approx. 21 nm and yield a *deviation from the mean* of  $\pm 5$  mHz. Note that the wavelength span that could be used for the measurement is currently limited by the gain bandwidth of an EDFA, which had to be used to amplify the reference comb to have sufficient power to run three BDUs simultaneously. The results for different gate times and for the two different counting methods are shown in Table 1 (the complete list is contained in the supplementary information). The weighted average of these results verifies the uniformity of the comb spacing to a level of  $7.3 \times 10^{-18}$  (when referenced to the optical carrier). Normalized to the bandwidth of the measured Kerr lines (2.1 THz), this corresponds to  $5.2 \times 10^{-16}$ . This accuracy is on par with measurements for fiber based frequency combs[26] and confirms that the generated Kerr combs exhibit uniform mode spacing.

Next we investigated the role of dispersion underlying the observed comb generation. Dispersion in whispering-gallery-mode (WGM) microcavities is characterized by the deviation in the free spectral range  $\Delta\nu_{\text{FSR}} = (\nu_{m+1} - \nu_m) - (\nu_m - \nu_{m-1}) = \nu_{m+1} - \nu_{m-1} - 2\nu_m$  and has two contributions. Geometrical dispersion accounts for a negative FSR dispersion, given by  $\Delta\nu_{\text{FSR}} \approx -0.41 \frac{c}{2\pi \cdot n \cdot R} \cdot m^{-5/3}$  where  $R$  the cavity radius (cf. supplementary information). Material dispersion on

$\tau(s)$	N	Mean (mHz)	$\sigma(mHz)$	$\epsilon$	Technique
1	3493	$-0.9 \pm 5.5$	322	$2.7 \times 10^{-17}$	2 Counters
3	173	$5.8 \pm 12.6$	165	$6.3 \times 10^{-17}$	Ratio
10	22	$-17.9 \pm 15.0$	70	$7.5 \times 10^{-17}$	Ratio
30	39	$1.7 \pm 7.4$	46	$3.7 \times 10^{-17}$	Ratio
100	42	$-0.3 \pm 2.7$	17	$1.4 \times 10^{-17}$	Ratio
300	14	$-0.8 \pm 2.8$	11	$1.4 \times 10^{-17}$	Ratio

TABLE I: Summary of the experimental results on the accuracy of the mode spacing. The weighted mean of all measurements (including SI) yields a relative accuracy of  $7.3 \times 10^{-18}$ .

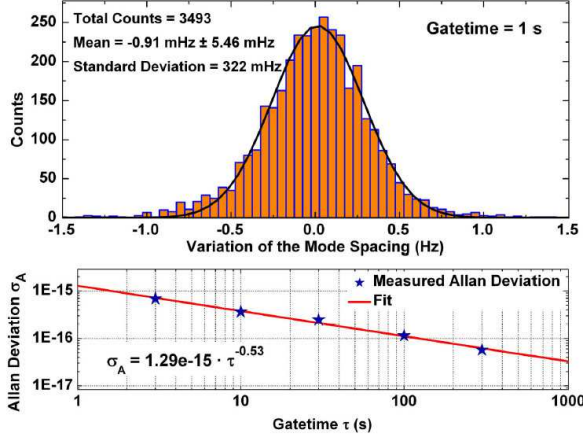


FIG. 4: Frequency counting experiment. Panel (A): The deviation from equidistant mode spacing for a gate time of 1 second for the parametric spectrum and measurement setup described in Fig 3. For this measurement 3493 points were recorded. The solid red line is a Gaussian fit to the distribution. The deviation from the mean implies an accuracy of the mode spacing at the mHz level, confirming the comb like structure of the parametric spectrum. Panel (B): Allan deviation as a function of gate time, exhibiting an inverse square-root dependence on the gate time, as determined by the fit (solid red line).

the other hand is given by  $\Delta\nu_{FSR} \approx \frac{1}{4\pi^2} \frac{c^2 \lambda^2}{n^3 R^2} \cdot GVD$ , where  $GVD = -\frac{\lambda}{c} \frac{\partial^2 n}{\partial \lambda^2}$  is the group velocity dispersion parameter. Since the GVD of silica is positive for wavelength greater than  $1.3 \mu\text{m}$  (anomalous dispersion), it can compensate the intrinsic resonator dispersion (causing  $\Delta\nu_{FSR} > 0$ ). Indeed we measured a positive dispersion (cf. SI) which equates to only ca. 20 MHz over a span of ca. 60 nm. This low value indicates that the present experiments are carried out close to the zero dispersion wavelength, in agreement with theoretical predictions.

Note that the residual cavity dispersion exceeding the “cold” cavity linewidth does not preclude the parametric comb generation process. This can be explained in terms of a nonlinear optical mode pulling process as reported in Ref. [14]. The strong CW pump laser will in-

duce both self-phase modulation (SPM) and cross-phase modulation (XPM)[28], the latter being twice as large as the former. The resultant XPM and SPM induced refractive index changes will shift the cavity resonance frequencies by different amounts, thereby causing a net change in the (driven) cavity dispersion from its *passive* (un-driven) value[14]. This nonlinear mode pulling can provide a mechanism to compensate the residual cavity dispersion.

Regarding future experimental work in light of applications in metrology, we note that absolute referencing can be attained by locking the pump laser to a known atomic transition and locking the mode spacing to a microwave reference (such as a Cs atomic clock). The latter requires that the two degrees of freedom of the comb, its repetition rate (i.e. mode spacing,  $\Delta\nu$ ) and frequency offset, i.e.  $\nu_{CEO} = (\nu_0 \bmod \Delta\nu)$  to be controlled independently. Indeed it could already been shown in a proof of concept experiment that it is possible to lock two modes of the Kerr comb simultaneously to two modes of the reference comb, showing that we are able to control both  $\nu_{CEO}$  and  $\Delta\nu$ . The two actuators used for this lock are the detuning of the pump laser from the microcavity resonance and the pump power, which affects the optical pathlength of the cavity via the thermal effect and the nonlinear phase shift.

Pertaining to the implications of our work, we note that the present observation of a monolithic frequency comb generator could potentially prove useful for frequency metrology, given however further improvements. Evidently a readily measurable repetition rate would prove useful when directly referencing the optical field to a microwave signal[2]. To this end a  $660\text{-}\mu\text{m}$ -diameter microcavity would already allow operating at repetition rates  $< 100 \text{ GHz}$ , which can be detected using fast photodiodes. On the other hand, a large mode spacing as demonstrated here could prove useful in several applications, such as line-by-line pulse shaping, calibration of astrophysical spectrometers or direct comb spectroscopy. The high repetition rate from an on chip device may also prove useful for the generation of multiple channels for high capacity telecommunications (spacing 160 GHz) and for the generation of low noise microwave signals. Furthermore, we note that parametric interactions do also occur in other types of microcavities - e.g.  $\text{CaF}_2$ [15] - provided the material exhibits a third order nonlinearity and sufficiently long photon lifetimes. As such the cavity geometry is not conceptually central to the work and the reported phenomena should become equally observable in other types of high-Q microresonators, such as silicon, SOI or crystalline based WGM-resonators. Indeed the recent observation of net parametric gain[29] on a silicon chip is a promising step in this direction.

*Acknowledgements:* The authors thank T. W. Hänsch, Th. Udem, K. J. Vahala and Scott Diddams for critical discussions and suggestions. TJK acknowledges support via an Independent Max Planck Junior Research Group.



This work was funded as part of a Marie Curie Excellence Grant (MEXT-CT-2006-042842), the DFG funded Nanoscience Initiative Munich (NIM) and a Marie Curie

Reintegration Grant (MIRG-CT-2006-031141). The authors gratefully acknowledge J. Kotthaus for access to clean-room facilities for sample fabrication.

- 
- [1] T. Udem, R. Holzwarth, and T. W. Hansch. Optical frequency metrology. *Nature*, 416(6877):233–237, March 2002.
  - [2] S. T. Cundiff and J. Ye. Colloquium: Femtosecond optical frequency combs. *Reviews Of Modern Physics*, 75(1):325–342, January 2003.
  - [3] S. T. Ye, J. & Cundiff. *Femtosecond Optical Frequency Comb: Principle, Operation and Applications*. Springer, 2005.
  - [4] R. J. Jones, K. D. Moll, M. J. Thorpe, and J. Ye. Phase-coherent frequency combs in the vacuum ultraviolet via high-harmonic generation inside a femtosecond enhancement cavity. *Physical Review Letters*, 94(19):193201, May 2005.
  - [5] C. Gohle, T. Udem, M. Herrmann, J. Rauschenberger, R. Holzwarth, H. A. Schuessler, F. Krausz, and T. W. Hansch. A frequency comb in the extreme ultraviolet. *Nature*, 436(7048):234–237, July 2005.
  - [6] S. A. Diddams, D. J. Jones, J. Ye, S. T. Cundiff, J. L. Hall, J. K. Ranka, R. S. Windeler, R. Holzwarth, T. Udem, and T. W. Hansch. Direct link between microwave and optical frequencies with a 300 THz femtosecond laser comb. *Physical Review Letters*, 84(22):5102–5105, May 2000.
  - [7] S. A. Diddams, T. Udem, J. C. Bergquist, E. A. Curtis, R. E. Drullinger, L. Hollberg, W. M. Itano, W. D. Lee, C. W. Oates, K. R. Vogel, and D. J. Wineland. An optical clock based on a single trapped  $\text{Hg-199}(+)$  ion. *Science*, 293(5531):825–828, August 2001.
  - [8] M. J. Thorpe, K. D. Moll, R. J. Jones, B. Safdi, and J. Ye. Broadband cavity ringdown spectroscopy for sensitive and rapid molecular detection. *Science*, 311(5767):1595–1599, March 2006.
  - [9] S. A. Diddams, L. Hollberg, and V. Mbele. Molecular fingerprinting with the resolved modes of a femtosecond laser frequency comb. *Nature*, 445(7128):627–630, February 2007.
  - [10] M. Kourogi, K. Nakagawa, and M. Ohtsu. Wide-span optical frequency comb generator for accurate optical frequency difference measurement. *Ieee Journal Of Quantum Electronics*, 29(10):2693–2701, October 1993.
  - [11] J. Ye, L. S. Ma, T. Day, and J. L. Hall. Highly selective terahertz optical frequency comb generator (vol 22, pg 301, 1997). *Optics Letters*, 22(10):746–746, May 1997.
  - [12] D. J. Jones, S. A. Diddams, J. K. Ranka, A. Stentz, R. S. Windeler, J. L. Hall, and S. T. Cundiff. Carrier-envelope phase control of femtosecond mode-locked lasers and direct optical frequency synthesis. *Science*, 288(5466):635–639, April 2000.
  - [13] D. K. Armani, T. J. Kippenberg, S. M. Spillane, and K. J. Vahala. Ultra-high-Q toroid microcavity on a chip. *Nature*, 421(6926):925–928, February 2003.
  - [14] T. J. Kippenberg, S. M. Spillane, and K. J. Vahala. Kerr-nonlinearity optical parametric oscillation in an ultrahigh-Q toroid microcavity. *Physical Review Letters*, 93(8):083904, August 2004.
  - [15] A. A. Savchenkov, A. B. Matsko, D. Strekalov, M. Mohageg, V. S. Ilchenko, and L. Maleki. Low threshold optical oscillations in a whispering gallery mode  $\text{CaF}_2$  resonator. *Physical Review Letters*, 93(24):243905, December 2004.
  - [16] G. Steinmeyer, D. H. Sutter, L. Gallmann, N. Matuschek, and U. Keller. Frontiers in ultrashort pulse generation: Pushing the limits in linear and nonlinear optics. *Science*, 286(5444):1507–1512, November 1999.
  - [17] U. Keller. Recent developments in compact ultrafast lasers. *Nature*, 424(6950):831–838, August 2003.
  - [18] A. M. Weiner. Femtosecond pulse shaping using spatial light modulators. *Review Of Scientific Instruments*, 71(5):1929–1960, May 2000.
  - [19] M. T. et al. Murphy. High-precision wavelength calibration with laser frequency combs. *arXiv:astro-ph/0703622*, 2007.
  - [20] K. J. Vahala. Optical microcavities. *Nature*, 424(6950):839–846, August 2003.
  - [21] A. J. Chang, R. K. & Campillo. *Optical processes in microcavities*. World Scientific, 1996.
  - [22] M. H. Dunn and M. Ebrahimzadeh. Parametric generation of tunable light from continuous-wave to femtosecond pulses. *Science*, 286(5444):1513–1517, November 1999.
  - [23] T. Carmon and K. J. Vahala. Visible continuous emission from a silica microphotonic device by third-harmonic generation. *Nature Physics*, 3(6):430–435, June 2007.
  - [24] R. H. Stolen and J. E. Bjorkholm. Parametric amplification and frequency-conversion in optical fibers. *Ieee Journal Of Quantum Electronics*, 18(7):1062–1072, 1982.
  - [25] S. M. Spillane, T. J. Kippenberg, O. J. Painter, and K. J. Vahala. Ideality in a fiber-taper-coupled microresonator system for application to cavity quantum electrodynamics. *Physical Review Letters*, 91(4):043902, July 2003.
  - [26] P. Kubina, P. Adel, F. Adler, G. Grosche, T. W. Hansch, R. Holzwarth, A. Leitenstorfer, B. Lipphardt, and H. Schnatz. Long term comparison of two fiber based frequency comb systems. *Optics Express*, 13(3):904–909, February 2005.
  - [27] A. Schliesser, M. Brehm, F. Keilmann, and D. W. van der Weide. Frequency-comb infrared spectrometer for rapid, remote chemical sensing. *Optics Express*, 13(22):9029–9038, October 2005.
  - [28] G.P. Agrawal. *Nonlinear Fiber Optics*. Academic Press, 2006.
  - [29] M. A. Foster, A. C. Turner, J. E. Sharping, B. S. Schmidt, M. Lipson, and A. L. Gaeta. Broad-band optical parametric gain on a silicon photonic chip. *Nature*, 441(7096):960–963, June 2006.
  - [30] T. J. Kippenberg, S. M. Spillane, and K. J. Vahala. Demonstration of ultra-high-Q small mode volume toroid microcavities on a chip. *Applied Physics Letters*, 85(25):6113–6115, December 2004.
  - [31] T. Carmon, L. Yang, and K. J. Vahala. Dynamical thermal behavior and thermal self-stability of microcavities.

- Optics Express*, 12(20):4742–4750, October 2004.
- [32] T. J. Kippenberg, S. M. Spillane, and K. J. Vahala. Modal coupling in traveling-wave resonators. *Optics Letters*, 27(19):1669–1671, October 2002.
- [33] S. Schiller. Asymptotic-expansion of morphological resonance frequencies in Mie scattering. *Applied Optics*,

- 32(12):2181–2185, April 1993.
- [34] Tobias Kippenberg. *Nonlinear Optics in Ultra-high-Q Whispering-Gallery Optical Microcavities*. PhD thesis, California Institute of Technology, 2004.

## I. GENERATION OF KERR COMBS AT LOWER REPETITION RATES

Figure 5 shows the Kerr comb spectrum at a lower repetition rate mentioned in the main paper. The repetition rate is 375 GHz, corresponding to a free spectral range of 3 nm. With larger samples it should be possible to generate repetition rates smaller than 100 GHz which permits the direct measurement of the repetition rate with high-bandwidth photodiodes.

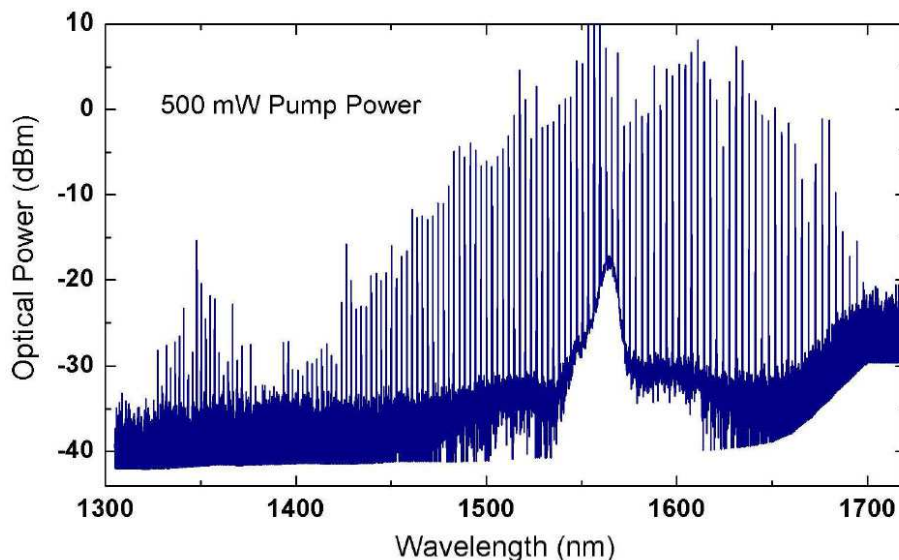


FIG. 5: Kerr comb generated in an 177- $\mu\text{m}$ -diameter toroid. The total power in the spectrum (pump line + generated sidebands) is around 500 mW distributed over more than 134 lines. The free spectral range is 3 nm.

## II. BEAT NOTE EXPERIMENTS BETWEEN THE FIBER LASER COMB AND KERR COMB

To demonstrate the equidistant nature of the parametric Kerr lines, a reference frequency comb in the form of a mode locked erbium fiber laser is used (from Menlo Systems GmbH). The principle underlying the measurement is similar to the concept of multi-heterodyne spectroscopy[27]. Assuming that the reference comb produces a spectrum with frequencies  $f_{\text{ceo}} + n \cdot f_{\text{rep}}$  (where  $f_{\text{rep}}$  is the repetition rate,  $f_{\text{ceo}}$  is the carrier envelope offset frequency and  $n$  is an integer number of order  $2 \cdot 10^6$ ) and the Kerr comb produces frequencies  $\nu_0 + m \cdot \Delta\nu$  ( $m$  integer), the signal generated by interfering the two combs will have an imprinted radio frequency (RF) beat note spectrum. If the reference comb's repetition rate is adjusted such that a multiple of it is close to the Kerr mode spacing, i.e.  $m_0 \cdot f_{\text{rep}} \approx \Delta\nu$  (with an integer  $m_0$ ), then the  $N$  different Kerr comb lines will generate  $N$  different RF beat notes which will again be evenly spaced, i.e. their frequencies are  $f_0 + \Delta f \cdot k$  (with  $\Delta f = (\Delta\nu \bmod f_{\text{rep}})$  and  $k$  integer).

The experimental setup is depicted in Figure 2 of the main paper. A tunable external cavity diode laser (ECDL) is used to pump a microtoroid resonance as detailed in [30] and [14]. Since the cavity resonances are polarization dependent, a in-fiber polarization controller is used to adjust the polarization of the pump laser. The microtoroid is placed in a sealed enclosure containing a nitrogen atmosphere, to avoid the deposition of water on the surface of the silica toroid which has strong absorption bands in the 1550-nm regime. In the microresonator a spectrum of modes is generated via nonlinear parametric interactions and four-wave mixing (see main paper). The output signal of the tapered optical fiber (containing the parametric modes that are outcoupled from the microresonator back to

the tapered fiber) is split by two 3 dB couplers and monitored with a photodiode connected to an oscilloscope and an optical spectrum analyzer. Another fraction of the taper output is sent to a “beat detection unit” (BDU) and superimposed with a fiber-laser-based reference frequency comb with a repetition rate of 100 MHz[26]. The BDU consists of quarter wave plates and half wave plates to prepare orthogonal linear polarization in the two input beams, which are subsequently combined using a polarizing beam splitter. By means of a half-wave plate, an adjustable linear combination of the two input beams’ polarizations is then rotated onto the transmission axis of a polarizer, where the two input beams interfere. To increase the signal-to-noise ratio (SNR), the spectral region containing the Kerr comb lines is selected by a grating and finally detected with a PIN InGaAs photodiode (Menlo Systems FPD 510). An oscilloscope with a built-in FFT routine is utilized to analyze the radio frequency spectrum. For rough analysis an electronic spectrum analyzer is used. Since the repetition rate of the reference comb is around 100 MHz the beat note frequencies between a laser line and the reference comb are in the range of 0 MHz to 50 MHz. Now the repetition rate of the reference comb is adjusted until  $(\Delta\nu \bmod f_{\text{rep}})$  is a small frequency such that for all  $k$  of interest the condition  $0 < f_0 + k \cdot \Delta f < f_{\text{rep}}/2$  is fulfilled. The observation of an equidistant RF beat “comb” then provides proof for the equidistance of the Kerr comb.

### III. MEASURING THE ACCURACY OF THE MODE SPACING USING HETERODYNE SPECTROSCOPY

#### A. Measuring with two counters

To verify the equidistance of the Kerr comb modes it is necessary to know the frequencies of three Kerr comb modes simultaneously. The frequency counting is achieved by using radio frequency counters that are connected to a photodiode in a beat note detection unit (cf. figure 2 in the main paper). To determine the frequencies of three Kerr comb modes at the same time, three beat note detection units (BDU) have been built. By tuning the grating of the BDUs it is possible to measure the beat note frequency of a single Kerr comb line with a reference comb line. For simplicity reasons, one BDU is used to lock the diode laser pumping the microcavity to a single mode of the reference comb. Additionally the repetition rate of the reference comb is locked to a frequency of around 100 MHz, stabilized by a 10 MHz frequency standard generated by an in-house hydrogen maser. The two remaining beat detection units are placed at the output of the microcavity and the gratings are adjusted in a way that each of them counts a different Kerr comb mode. Note that the output of the reference comb had to be amplified with an EDFA to obtain sufficient power to run three BDUs simultaneously (a single line of the reference comb contains ca. 10 nW optical power). With this setup it was possible to achieve signal-to-noise ratios for the Kerr sideband beat notes of more than 30 dB at a resolution bandwidth of 500 kHz (Additional RF filters with a 3-dB-bandwidth of 3 MHz have been used to filter out background noise). In the present experiment we focused on counting the 5<sup>th</sup> (beat note frequency  $f_1$ ) and the 7<sup>th</sup> Kerr comb sideband (beat note frequency  $f_2$ ), whereas the pump laser was phase locked to the fiber laser reference comb such that its beat with the reference comb was fixed to a frequency  $f_0$ . Note that the pump laser already constitutes one tooth of the Kerr comb. For an equally spaced Kerr comb we therefore expect  $f_1 = f_0 + N \cdot \Delta f$  and  $f_2 = f_0 + M \cdot \Delta f$  with  $N = 5$  and  $M = 7$  to be the beat note frequencies of the sidebands. The variation of the mode spacing  $\epsilon$  of the Kerr comb is given by

$$\epsilon = \frac{f_2 - f_1}{M - N} - \frac{f_1 - f_0}{N} \quad , \quad (1)$$

which is zero for an equally spaced comb. With the measured values for  $f_1$  and  $f_2$  and the known frequency  $f_0$  it is possible to calculate the variation of the mode spacing  $\epsilon$ . The two counters are referenced to the same frequency standard as the offset lock for the pump laser and are externally triggered with a signal from a pulse generator. This external triggering was necessary since the mode spacing of the Kerr comb was fluctuating by approximately 40 kHz r.m.s., giving rise to “breathing” of the Kerr comb modes(cf. figure 6). Hence, it proved critical for a high accuracy that the two counters measured simultaneously, to allow the cancellation of the common fluctuations.

#### B. Measuring the ratio of the distance to the sidebands

To avoid the synchronization problems mentioned before, the experimental setup depicted in figure 7 was used. In brief, the three counter signals were first electronically mixed with  $f_0$  and filtered yielding only the distance between pump and the N<sup>th</sup> (M<sup>th</sup>) Kerr-sidebands. With this setup, a slightly smaller standard deviation of the measurements could be achieved by using just one counter with two inputs to measure the ratio  $R$  of the distance between the pump

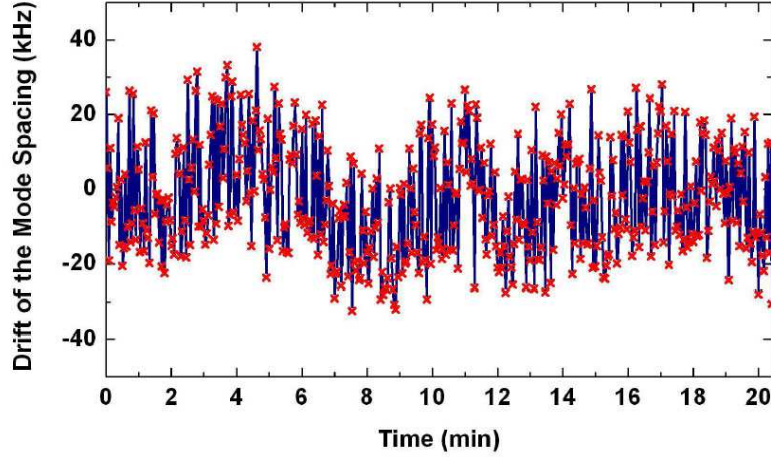


FIG. 6: Drift of the mode spacing of the Kerr comb when not stabilized. The mode spacing exhibits fluctuations of approximately 40 kHz for short time scales and some slower thermal drifts for time scales of several minutes. Note that these fluctuations of the mode spacing do not affect the equidistance of the modes of the Kerr comb since they are fluctuating simultaneously.

beat and the two sideband beats,

$$R = \frac{f_2 - f_0}{f_1 - f_0}. \quad (2)$$

Solving this for  $f_2$  and using equation 1 we obtain the dependence of the variation of the mode spacing  $\epsilon$  from the ratio  $R$ :

$$\epsilon = \frac{f_1 - f_0}{M - N} \cdot R + (f_0 - f_1) \cdot \left( \frac{1}{M - N} + \frac{1}{N} \right) \quad (3)$$

Using the frequency difference  $f_1 - f_0$ , which was set to approximately 10 MHz, it is possible to derive the variation of the mode spacing  $\epsilon$  by measuring the frequency ratio  $R$ .

#### IV. EXPERIMENTAL RESULTS OF THE COUNTER MEASUREMENTS

Table II shows the experimental results from the measurements of the Kerr comb equidistance. Note that a total of 9 data points out of the 8382 measurements from table II have been removed from analysis. These data points have been separated by the other data points of the respective measurements by more than 15 standard deviations. Assuming a Gaussian distribution (which was indeed found for the remaining 8373 measurements) the probability of measuring a point 15 standard deviations off as given by the cumulative error function is  $(1 - \text{erf}(15/\sqrt{2})) \approx 7.3 \times 10^{-51}$ . These points are believed to originate from some local perturbations in the lab leading to a temporary reduction of the signal-to-noise level of the radio frequency beat notes. The weighted mean  $\bar{\epsilon}_w$  in table II has been calculated with the inverse squared standard error of the mean as weight:

$$\bar{\epsilon}_w = \frac{\sum \epsilon / \sigma_\epsilon^2}{\sum 1 / \sigma_\epsilon^2} \quad (4)$$

$$\sigma_{\epsilon_w}^2 = \frac{1}{\sum 1 / \sigma_\epsilon^2} \quad (5)$$

The weighted mean calculated from all measurements leads to a variation of the modespacing of  $\bar{\epsilon}_w = -0.8 \text{ mHz} \pm 1.4 \text{ mHz}$ . Normalized to the optical carrier frequency of 192 THz, this leads to an accuracy of the equidistance of  $7.3 \times 10^{-18}$ .



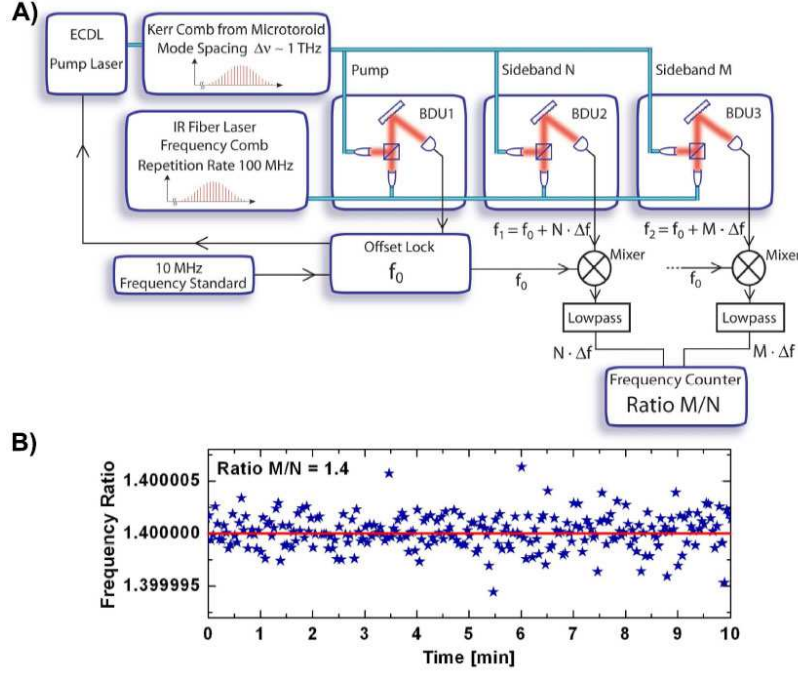


FIG. 7: Panel A). Experimental setup to measure the ratio of the frequency separation between pump laser and two different Kerr comb sidebands. ECDL = External Cavity Diode Laser. Beat note detection unit 1 (BDU1) is used to phase lock the pump laser line from the Kerr comb to the reference comb with an offset frequency  $f_0$ . BDU2 (BDU3) is adjusted to measure the beat note frequency between the  $N^{th}$  ( $M^{th}$ ) Kerr comb line and the reference comb. By mixing these frequencies down with the offset lock frequency  $f_0$  using electronic mixers, new frequencies  $N \cdot \Delta f$  and  $M \cdot \Delta f$  are generated. The ratio of these frequencies is  $M/N = 1.4$  for the  $7^{th}$  and the  $5^{th}$  sideband. Panel B) shows a measurement of the frequency ratio of the radio frequency beat notes generated from the  $7^{th}$  and the  $5^{th}$  sideband of the Kerr comb.

## V. MEASUREMENT OF CAVITY DISPERSION

To measure cavity dispersion, we employ the arrangement shown in figure 8. In brief, we first lock an external cavity laser around 1550 nm to one of the fundamental WGM cavity modes (the same resonance that gives rise to cascaded sidebands at higher power). The cavity resonance of the monolithic microresonator is locked to the external cavity laser by virtue of the thermal self locking technique[31]. The power is chosen to be far below the parametric threshold  $< 85 \mu\text{W}$  but sufficient to entail a stable lock. Next, the frequency comb is offset-locked to the external cavity laser by recording the beat note signal in a separate beat note detection unit (for working principle of the beat detection unit see last section). To achieve stable locking the generated beating is filtered and amplified yielding a SNR of ca. 25 – 30 dB (at a resolution bandwidth of 400 kHz). For dispersion measurement the frequency comb must be locked at an arbitrary detuning with respect to the ECDL. The latter is accomplished by mixing the beat note with a (variable) reference signal ( $f_{\text{offset}}$ ) down to 10 MHz and implementing a phase lock with feedback on the fiber comb's repetition rate ( $f_{\text{rep}}$ ) by controlling the cavity length using a mirror mounted on a piezoelectric tube (Note that all RF generators and analyzers are stabilized using an in-house 10-MHz-reference). Owing to the fact that the cavity linewidth is  $< 5$  MHz and the repetition rate of the fiber comb (FC) is 100 MHz, not more than *one* FC comb mode at a time can be resonant with one microresonator mode. Since measuring the coupling of an individual comb mode into the resonator in transmission is difficult, we measure the reflection of the cavity induced by modal coupling[32]. By variation of  $f_{\text{offset}}$  (and by recording simultaneously  $f_{\text{rep}}$ ) this allows to resolve the linewidth of individual cavity modes in reflection when using an OSA in zero-span mode. Hence this measurement provides an accurate means to measure frequency gap (free spectral range) between two cavity resonances  $\nu_m$  and  $\nu_{m+\Delta m}$  modulo the repetition rate of the fiber comb ( $(\nu_m - \nu_{m+\Delta m}) \bmod f_{\text{rep}}$ ). The low power of the individual FC lines (ca. 10 nW) ensures that the probed cavity mode is not thermally distorted. To remove the ambiguity in the number of comb lines ( $n$ ) between the FSR of the cavity i.e.  $n = \lfloor (\nu_m - \nu_{m+\Delta m}) / f_{\text{rep}} \rfloor$  a second measurement was carried out with a different repetition rate, which allowed to retrieve  $n$ . So the actual free spectral range between two cavity resonances can be derived by:

$$\nu_{\text{FSR}} = f_{\text{beatnote}} + n \cdot f_{\text{rep}}$$

Gate time (s)	Readings	Mean Value for $\epsilon$ (mHz)	StdDev of $\epsilon$ (Hz)	Counting Method
0.03	217	$-33 \pm 556$	8.2	ratio
0.1	223	$-80 \pm 181$	2.7	ratio
0.3	293	$2.4 \pm 50.1$	0.86	ratio
1	3493	$-0.91 \pm 5.46$	0.32	2 counters
1	3499	$3.9 \pm 10.1$	0.60	2 counters
1	98	$-40.1 \pm 27.4$	0.27	ratio
1	179	$8.0 \pm 25.5$	0.34	ratio
3	173	$5.8 \pm 12.6$	0.17	ratio
10	22	$-17.9 \pm 15.0$	0.070	ratio
30	39	$1.65 \pm 7.41$	0.046	ratio
60	72	$-1.88 \pm 3.00$	0.025	ratio
100	18	$1.12 \pm 5.98$	0.024	ratio
100	42	$-0.26 \pm 2.69$	0.017	ratio
300	14	$-0.82 \pm 2.83$	0.011	ratio
Weighted Mean $\bar{\epsilon}_w$ :		$-0.8 \text{ mHz} \pm 1.4 \text{ mHz}$	-	-

TABLE II: Complete list of the Kerr comb measurements with frequency counters. StdDev = standard deviation of the distribution. The last column shows the used method to acquire the data: “2 counters” stands for the measurements with two externally triggered counters (one for each Kerr sideband) and “ratio” stands for the method with one counter that directly measures the ratio between the distance between pump and two different Kerr comb lines (both methods are explained in the preceding section). As expected, the standard deviation of the measurements reduces with increasing gatetime. The total measurement time is 6 h 37 min.

Figure 9 shows the experimental result of the dispersion measurement. The used cavity had a free spectral range (FSR) of 7.9 nm, which corresponds to 0.96 THz. Plotted in figure 9 is the accumulated dispersion of the FSR, which we express for convenience as  $(\nu_{m+1} - \nu_m) - (\nu_1 - \nu_0)$ . Here, the  $\nu_m$  are the resonance frequencies of a “cold” microcavity. For this measurement,  $\nu_0$  is a resonance at 1585 nm (189 THz). From the graph it can be derived that the accumulated dispersion is 2.6 MHz per FSR (i.e. positive dispersion).

## VI. DISPERSION PREDICTIONS

The dispersion in our microcavities has two contributions. First, whispering-gallery mode microcavities exhibit an intrinsic variation of the free spectral range owing to the resonator geometry. The resonance frequency of the fundamental mode of a microsphere is approximately given by [33]

$$\nu_m = \frac{c}{2\pi n R} \left( m + 1/2 + \eta_1 \left( \frac{m + 1/2}{2} \right)^{1/3} + \dots \right), \quad (6)$$

where  $c$  is vacuum light speed,  $n$  the refractive index,  $R$  the cavity radius and  $\eta_1$  the first zero of the Airy function ( $\eta_1 \approx 2.34$ ). Hence, the variation of the free spectral range

$$\Delta\nu_{\text{FSR}} = (\nu_{m+1} - \nu_m) - (\nu_m - \nu_{m-1}) = \nu_{m+1} + \nu_{m-1} - 2\nu_m \approx \frac{\partial^2 \nu_m}{\partial m^2} \quad (7)$$

is given by

$$\Delta\nu_{\text{FSR}} = -\frac{c}{2\pi n R} \cdot \frac{\eta_1}{18} \left( \frac{m + 1/2}{2} \right)^{-5/3} \approx -0.41 \frac{c}{2\pi n R} m^{-5/3} < 0 \quad (8)$$

Evidently, the free spectral range *reduces* with increasing frequency corresponding to a negative group velocity dispersion (GVD), i. e. low frequency modes exhibit a shorter round trip time than high frequency modes. Supplementary figure S3 shows the variation for a 40- and 80-micron-radius microsphere.

A second contribution comes from the dispersion of the fused silica material constituting the resonator. Its contribution can be estimated by considering that the refractive index  $n$  is actually a function of frequency (and therefore

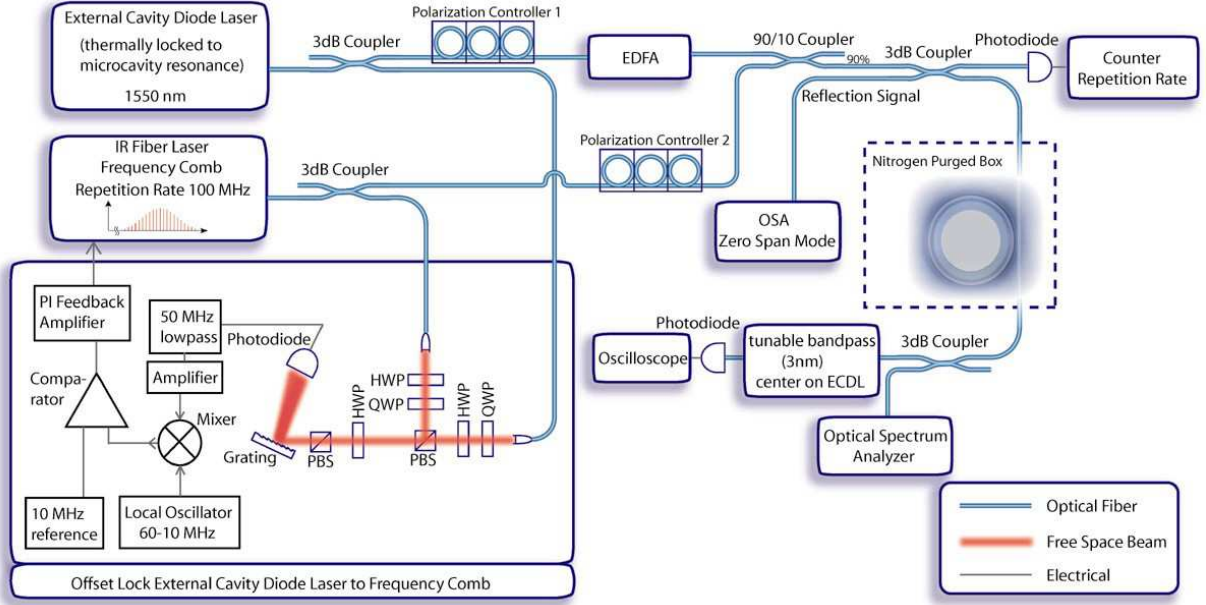


FIG. 8: Experimental setup of the dispersion measurement. The beat detection unit on the lower left side is used to establish an offset lock between the external cavity diode laser (ECDL) and the fiber laser frequency comb. Therefore the signal from the photodiode in the beat detection unit is first filtered with a 50 MHz lowpass to remove the strong signal of the 100 MHz repetition rate of the fiber laser comb. Subsequently the beat note signal is mixed down to 10 MHz with a variable frequency generator (10..60 MHz) and compared with a stable 10 MHz RF reference. The output of the comparator is sent to a PI feedback amplifier which is connected to a piezo-mechanical control of the repetition rate of the fiber laser. By adjusting the variable frequency generator one can change the distance between the laserline of the ECDL and the next comb line to an arbitrary value between 0 MHz and  $f_{\text{rep}}/2$ . The ECDL and the fiber comb are furthermore coupled to the microcavity with a microtoroid resonance thermally locked to the ECDL. To measure the distance between two cavity resonances an optical spectrum analyzer (OSA) in zero span mode is set to a wavelength of a different cavity resonance than the one pumped by the ECDL. Next, the offset lock is changed until a reflection signal of the fiber comb is detected on the OSA. Once this is achieved the ECDL and one mode of the fiber comb are on resonances with two different modes of the microcavity. This means the FSR can be derived as  $f_{\text{beatnote}} + n \cdot f_{\text{rep}}$ .

mode number  $m$ ),  $n \equiv n(m)$ . Neglecting geometric dispersion, the GVD of fused silica alone would lead to a FSR variation of

$$\Delta\nu_{\text{FSR}} \approx \frac{\partial^2}{\partial m^2} \left( \frac{c}{2\pi n(m)R} \cdot m \right) \approx \frac{c^2 \lambda^2}{4\pi^2 n^3 R^2} \cdot \text{GVD}, \quad (9)$$

where

$$\text{GVD} = -\frac{\lambda}{c} \frac{\partial^2 n}{\partial \lambda^2} \quad (10)$$

is the group-velocity dispersion of fused silica. This material parameter is well-known to change its sign in the 1300-nm wavelength region from about  $-100 \text{ ps/nm} \cdot \text{km}$  at 800 nm to  $+20 \text{ ps/nm} \cdot \text{km}$  at 1550 nm. Combining the two contributions, the positive sign of the GVD allows us in particular to cancel the geometric dispersion of our resonators to some extent, rendering the FSR nearly constant over a wide frequency span. Figure 10 displays the FSR variation for an 80- and 160-micrometer diameter microsphere, considering both material and geometric dispersion. Importantly, a zero dispersion point close to our operating wavelength occurs. Note that for a toroidal microcavity the location of the zero dispersion point is expected to be shifted to shorter wavelengths owing to the different resonator geometry. This expectation is borne out of finite element simulations showing that the resonance wavelength for a given  $m$  value is shorter in a microtoroid cavity as compared to a microsphere [34].

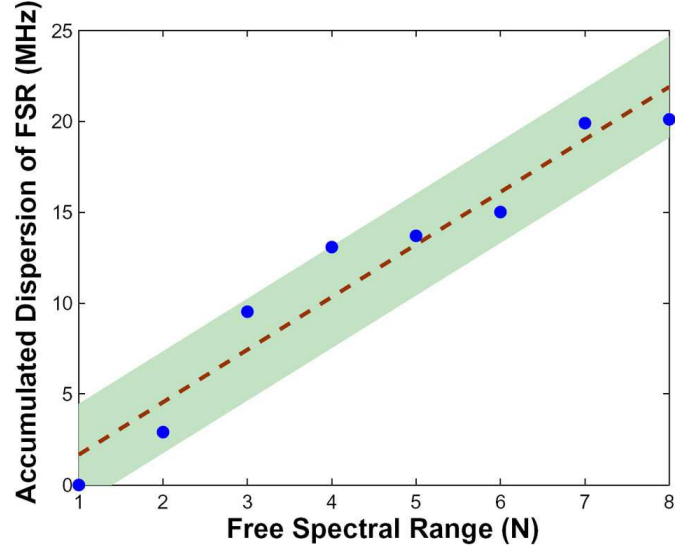


FIG. 9: Dispersion measurement of an 80- $\mu\text{m}$ -diameter monolithic microresonator. The figure shows the accumulated variation (i.e. dispersion) of the free spectral range i.e.  $(\nu_{m+1} - \nu_m) - (\nu_1 - \nu_0)$ . The variation of the FSR at higher frequencies (shorter wavelength) is referenced to the free spectral range recorded between 1577 nm ( $\nu_1$ ) and 1584 nm ( $\nu_0$ ). The shaded region denotes experimental uncertainty, the dotted line denotes a linear fit. As expected for a whispering-gallery mode dominated by material dispersion, the free spectral range increases for shorter wavelength.

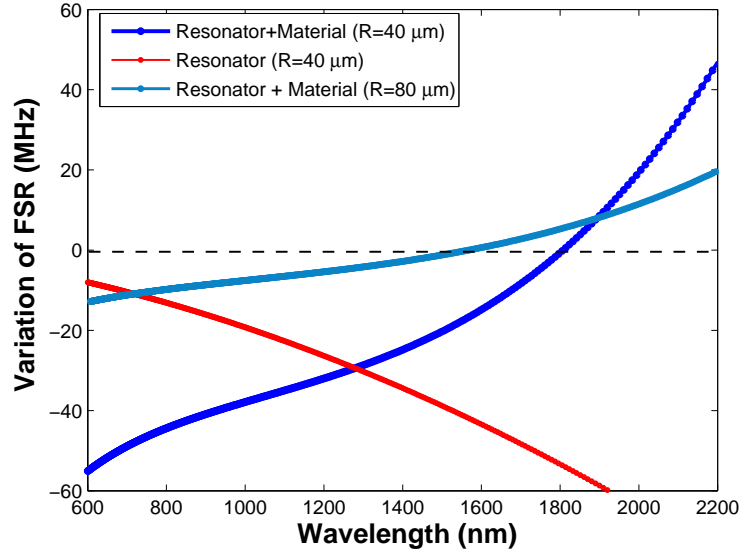


FIG. 10: Variation of the free spectral range of a whispering-gallery microsphere resonator (i.e.  $\Delta\nu_{\text{FSR}} = \nu_{m+1} + \nu_{m-1} - 2\nu_m$ ). Shown is the FSR dispersion for two resonator radii (40  $\mu\text{m}$  and 80  $\mu\text{m}$ ) including the effect of silica dispersion via the Sellmeier equation. Resonance locations were calculated using an asymptotic expansion of the microsphere resonance locations. Owing to the different signs of silica material and resonator dispersion, a zero dispersion point exists in the infrared.

## APPENDIX A: SYMBOLS USED THROUGHOUT THIS WORK

### Symbols Designation

$\nu_m$	Optical microcavity mode (with angular mode number $m$ )
$\nu_{\text{FSR}}$	Optical microcavity free spectral range ( $\nu_{\text{FSR}} =  \nu_m - \nu_{m+1} $ )
$\Delta\nu_{\text{FSR}}$	Optical microcavity variation of the free spectral range ( $\Delta\nu_{\text{FSR}} = \nu_{m+1} + \nu_{m-1} - 2\nu_m$ )
$\nu_{\text{ceo}}$	Kerr comb carrier envelope offset frequency
$\Delta\nu$	Kerr comb mode spacing
$f_{\text{rep}}$	Fiber reference comb repetition rate
$f_{\text{ceo}}$	Fiber reference comb carrier envelope frequency
$f_{0,1,2}$	Beat note unit (BDU) frequencies
$\Delta f$	Frequency spacing of the multi-heterodyne beat comb

---



